Available online at www.sciencedirect.com
ScienceDirect
Journal of Power Sources 175 (2008) 232–237
JOURNAL OF POWER SOURCES
www.elsevier.com/locate/jpowsour

Short communication

A new anode material for intermediate solid oxide fuel cells

Weitao Bao *, Hangmin Guan, Jihai Cheng

Department of Chemistry and Materials Engineering, Hefei University, Hefei 230022, China

Received 4 August 2007; received in revised form 28 August 2007; accepted 9 September 2007
Available online 15 September 2007

Abstract

A new anode material for intermediate temperature solid oxide fuel cells (IT-SOFCs) with a composite of $La_{0.7}Sr_{0.3}Cr_{1-x}Ni_xO_3$ (LSCN), CeO_2 and Ni has been synthesized. EDX analysis showed that 1.19 at% Ni was doped into the perovskite-type $La_{0.7}Sr_{0.3}CrO_3$ and Ce could not be detected in the perovskite phases. Results showed that the fine CeO_2 and Ni were highly dispersed on the $La_{0.7}Sr_{0.3}Cr_{1-x}Ni_xO_3$ substrates after calcining at 1450 °C and reducing at 900 °C. The thermal expansion coefficient (TEC) of the as-prepared anode material is 11.8×10^{-6} K^{-1} in the range of 30–800 °C. At 800 °C, the electrical conductivity of the as-prepared anode material calcined at 1450 °C for 5 h is 1.84 S cm^{-1} in air and 5.03 S cm^{-1} in an $H_2 + 3\%$ H_2O atmosphere. A single cell with yttria-stabilized zirconia (YSZ, 8 mol% Y_2O_3) electrolyte and the new materials as anodes and $La_{0.8}Sr_{0.2}MnO_3$ (LSM)/YSZ as cathodes was assembled and tested. At 800 °C, the peak power densities of the single cell was 135 mW cm^{-2} in an $H_2 + 3\%$ H_2O atmosphere.

Keywords: Anode; Doped-$LaCrO_3$; SOFCs

1. Introduction

Ni–cermet composites are the most commonly used materials as anodes for intermediate temperature solid oxide fuel cells (IT-SOFCs) [1–3]. In the popular Ni/YSZ cermet anode, although nickel has an excellent catalyst for hydrogen oxidation and good electrical current conductor [3], there are still some problems. First, cycling between oxidizing and reducing environments causes anode degradation due to the large Ni-NiO volume change. Such reduction–oxidation cycling may occur accidentally and cause catastrophic failure in SOFC systems. Second, less critical issues with Ni–YSZ anodes include the possibility of Ni-sintering at SOFC operating temperatures resulting in decreasing anode performance and the onset of creep in metals above 40% of the melting point (420 °C) for Ni. The above issues have motivated development of new Ni-free or reduced-Ni SOFC anode materials [4–6]. The replacement of Ni with another nonnoble metal for conductivity purposes is possible, but in order to realize redox stability it will likely be necessary to minimize the volume fraction of metallic phases that will inevitably exhibit considerable expansion and contraction upon redox cycling. Thus, electronically conducting ceramics, e.g., oxides based on lanthanum chromite and strontium titanate, are interesting as anode materials. These oxides are pure electronic conductors and have little electrocatalytic effect, as indicated by the relatively low power densities reported for anodes containing only these oxides [7]. To overcome this major drawback, two ways were used. First, the electronic conductor was mixed with the ionically conducting oxide [8,9]. More importantly, it was expected to enhance electrochemical performance by increasing the density of triple-phase boundaries. Second, 5 wt% of nanometer-scale NiO was added. A few recent reports have shown that the addition of small amounts of Ni to these oxide anodes decreased the anode polarization resistance and increased power density substantially [8–11].

Here we report results for SOFC anodes based on a composite containing $La_{0.7}Sr_{0.3}Cr_{1-x}Ni_xO_3$, CeO_2 and Ni. Results on anode microstructure and phases present are presented. In order to elucidate the performances, the electrical conductivity and the power density of a single cell using this material as the anode were measured.

2. Experimental

The new anode material with a general formula $(La_{0.7}Sr_{0.3})_{0.4}Ce_{0.6}Cr_{0.4}Ni_{0.6}O_3$ (LSCCN) was prepared by an

* Corresponding author. Tel.: +86 551 2158439; fax: +86 551 2158436.
E-mail address: bwt@hfuu.edu.cn (W. Bao).

0378-7753/$ – see front matter © 2007 Elsevier B.V. All rights reserved.
doi:10.1016/j.jpowsour.2007.09.026

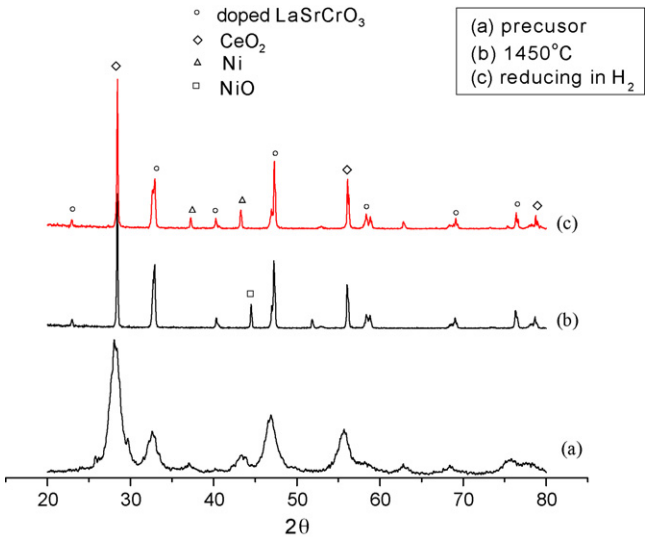

Fig. 1. The XRD patterns of the samples: (a) the precursor, (b) calcined at 1450 °C for 5 h, and (c) calcined at 1450 °C for 5 h and than reduced at 900 °C for 24 h in hydrogen atmosphere.

auto-ignition process. The starting substances are aqueous solutions of AR grade $Ce(NO_3)_3$, $La(NO_3)_3$, $Cr(NO_3)_3$, $Sr(NO_3)_2$, $Ni(NO_3)_2$ and citric acid. This forms a gel by heating at about 80 °C and wet gel was further heated to about 120 °C to remove the solvents. The dried gel was baked in an oven at 500–700 °C, where the combustion reaction took place within a few seconds to form the precursors. The powders were prepared by calcining the precursors at 1100–1500 °C for 2–5 h. The powders were characterized by an X-ray diffractometer (XRD) (D/max-rA, Rigaku). The samples were analyzed by scanning electron microscope (SEM, JEOL JSM-6400) equipped with EDX for compositional analysis. The shrinkage characteristics were observed using a Dilatometer (Netzsch, DIL 402 C) in an air atmosphere at an increase rate of 10 °C min^{-1}. The electrical conductivity of rectangular bar specimens (35 mm × 5 mm × 1.8 mm) calcined at 1450 °C for 5 h in air atmosphere was studied from 500 to 800 °C using standard DC four-probe technique (Model: 34401, H.P.).

For the electrolyte, we selected YSZ electrolyte. Commercially available YSZ powders were pressed into pellets under 200 MPa and were then calcined in air at 1400–1500 °C for 5 h to obtain a 350 μm thick YSZ electrolyte pellets with relative density greater than 97%. For the anode, the LSCCN–glycol slurry was coated onto one side of the YSZ electrolyte pellets, and then co-fired at 1350 °C for 2 h in air, so as to give an effective electrode area of 1 cm^2. For the cathode, we selected $La_{0.8}Sr_{0.2}MnO_3$ (LSM)/YSZ in a ratio 50/50 (wt%). LSM powders were prepared by the glycine-nitrate process and were mixed with YSZ. The LSM/YSZ powder is mixed with ethylene glycol to form a paste and applied onto another side of the

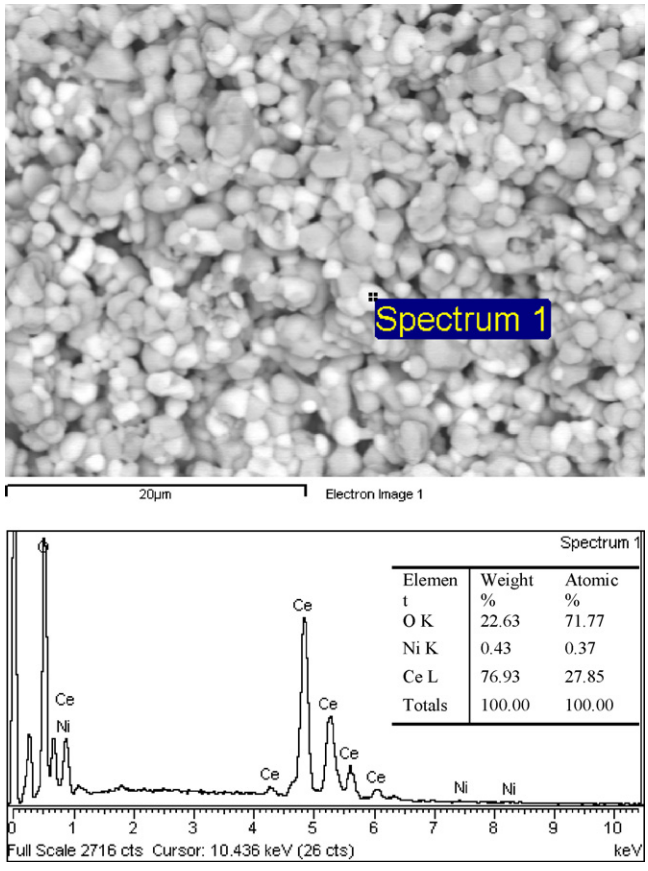

Fig. 2. EDX spectrum of LSCCN samples after reduced at 900 °C for 24 h in hydrogen atmosphere.

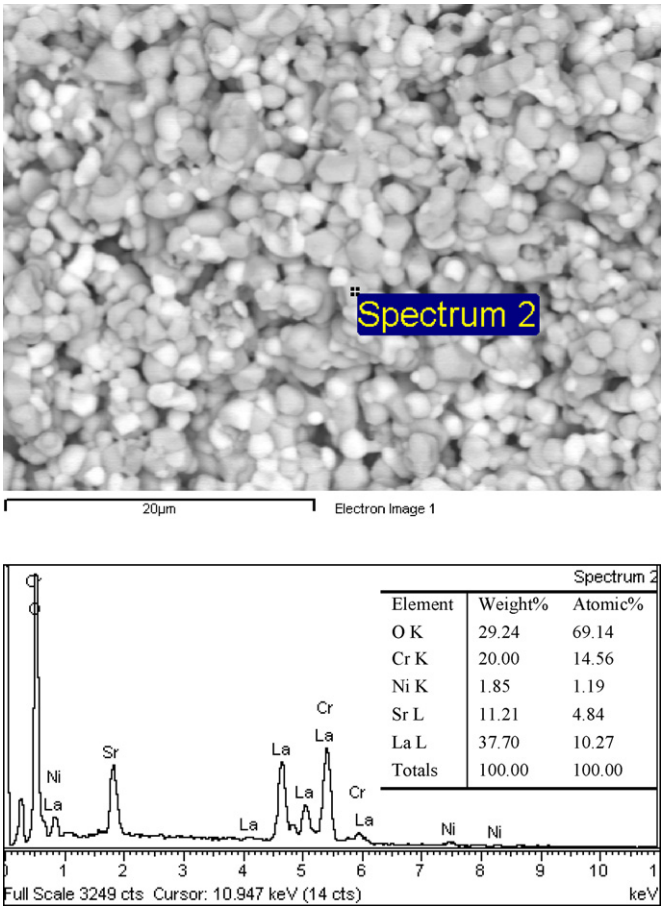

Fig. 3. EDX spectrum of LSCCN samples after reduced at 900 °C for 24 h in hydrogen atmosphere.

YSZ electrolyte pellets, and then co-fired at 1150 °C for 2 h in air to give the same effective electrode area of 1 cm^2. The single cell was sealed on an alumina tube with a silver paste (Heraeus 8710), and tested in a self-assembled cell testing system. Humidified (3% H_2O) hydrogen, which can be achieved by bubbling H_2 through water at about 25 °C, was used as fuel and stationary air as oxidant.

3. Results and discussion

The XRD patterns of the samples are shown in Fig. 1. The XRD pattern of the precursor sample (shown in Fig. 1a) suggests that the sample was not well crystallized, being mainly composed of the perovskite-type doped-$LaCrO_3$ phase, the fluorite type CeO_2 phase and NiO phase. After calcining at 1450 °C for 5 h, these phases were well crystallized (shown in Fig. 1b). The XRD pattern of the sample calcined at 1450 °C and than reduced at 900 °C for 24 h in hydrogen atmosphere is shown in Fig. 1c, where NiO is reduced into Ni. Comparing with Fig. 1b, there was no significant difference in peak width of the doped-$LaCrO_3$ and CeO_2 phases, indicating that these particle sizes did not increase significantly during reducing. In order to analyze the composition of the perovskite-type doped-$LaCrO_3$ phases, the EDX analysis is shown in Fig. 2. The white grain is CeO_2, and the CeO_2 grains with a size of about 0.2–1.0 μm are highly dispersed. Due to CeO_2 being a mixed conductor in a reducing fuel environment, a condition which should expand the reaction zone beyond the three phase boundaries, the highly dispersed CeO_2 phases should increase the activity of the anode for the electrochemical oxidation [12]. The grey grain is the

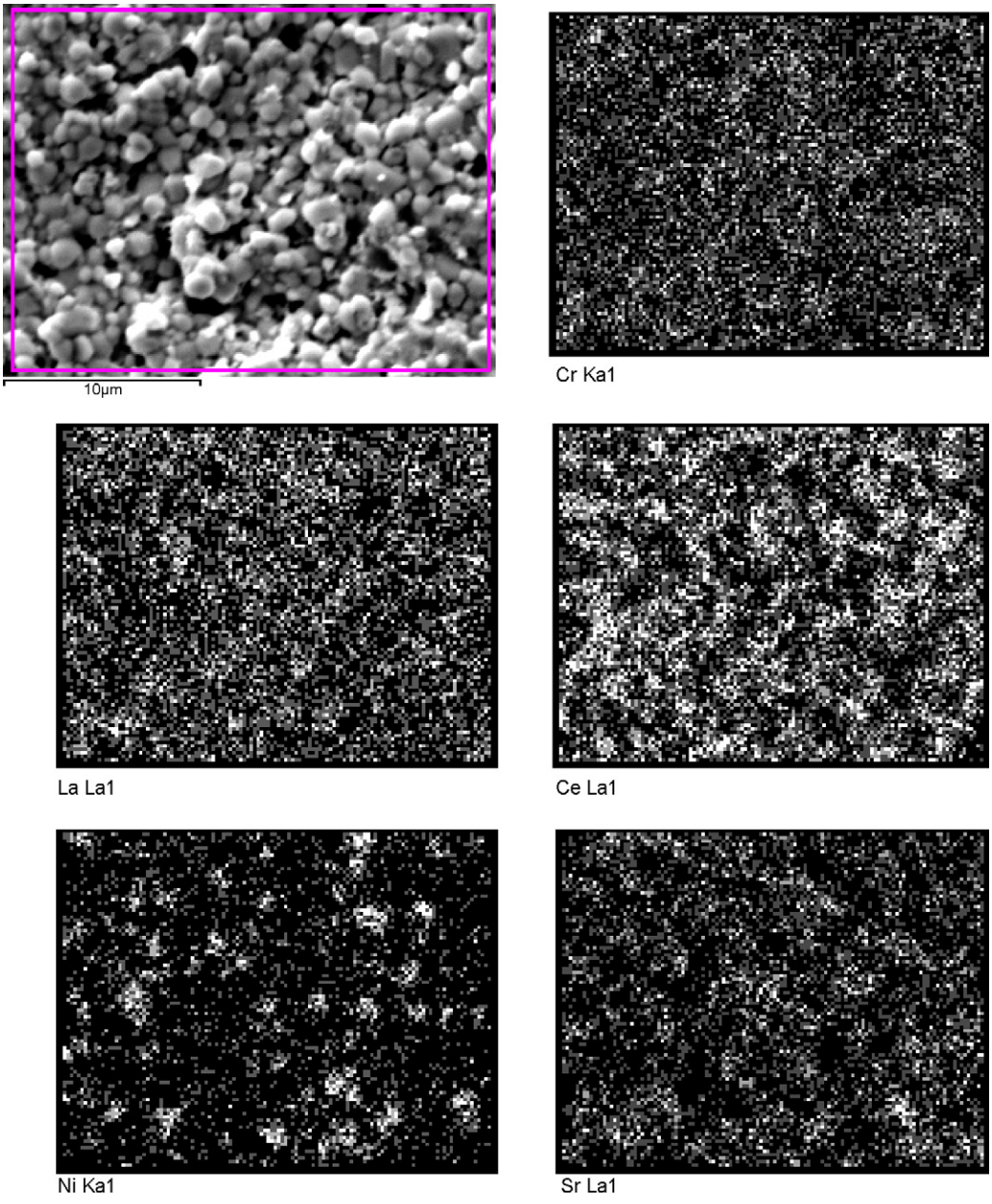

Fig. 4. SEM mapping of the LSCCN sample calcined at 1400 °C for 5 h in air and then reduced at 900 °C for 24 h in hydrogen atmosphere.

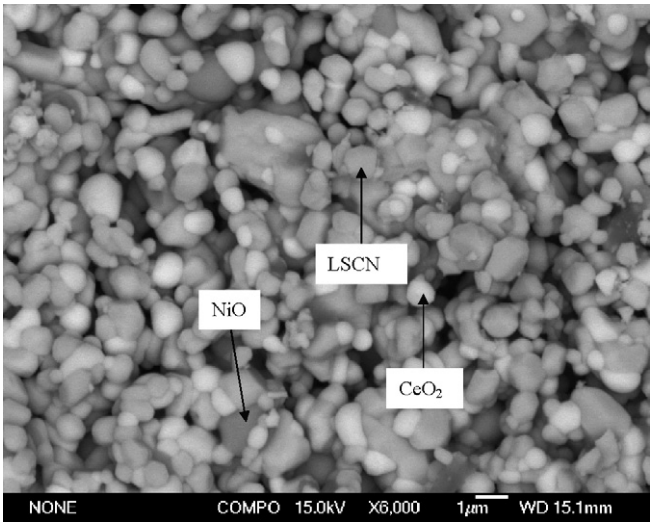

Fig. 5. An SEM image of the LSCCN sample calcined at 1450 °C for 5 h.

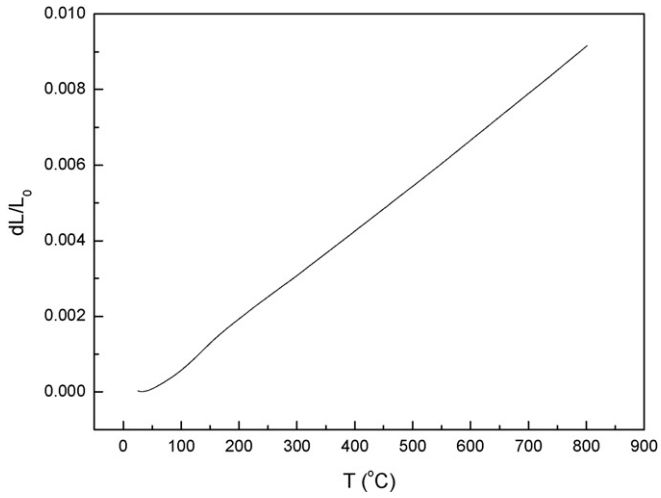

Fig. 7. Shrinkage characteristics of LSCCN sample after pre-calcining at 1450 °C for 5 h.

perovskite-type doped-$LaCrO_3$, the EDX analysis is shown in Fig. 3, in which there is 1.19 at% Ni to be doped and Ce was not detected in the perovskite phases. The doped-$LaCrO_3$ is called as $La_{0.7}Sr_{0.3}Cr_{1-x}Ni_xO_3$ (LSCN). As shown in Fig. 2, the higher temperature led to well-defined $La_{0.7}Sr_{0.3}Cr_{1-x}Ni_xO_3$ grains with a much larger size in the range of 0.5–2.0 μm. Fig. 4 shows the La, Sr, Ce, and Ni X-ray peak intensities versus position in the anode material calcined at 1450 °C for 5 h and then reduced at 900 °C for 24 h. Separate regions rich in La and Ce, corresponding to the LSCN and CeO_2 phases, respectively, were observed. Ni aggregations with a size of about 0.5–1.0 μm are homogeneously distributed. Ni appeared to be very fine and highly dispersed in the 1200 °C-calcined sample (not shown), indicating that Ni particles were small after low-temperature calcining, but coarsened during calcining at 1450 °C. An SEM image of the LSCCN sample calcined at 1450 °C for 5 h is given in Fig. 5. It was observed that CeO_2 grains have a homogeneous distribution, and NiO gains were surrounded by LSCN and CeO_2 grains. Good connections between NiO–LSCN, CeO_2–NiO and CeO_2–LSCN grains are important for fabricating a high-performance anode. Schematic of LSCN, CeO_2, and NiO phase formations is shown in Fig. 6. As shown schematically, LSCN formed a skeleton with well-connected CeO_2 and NiO homogenously distributed over the LSCN surfaces. NiO were surrounded by LSCN and CeO_2 grains. Such NiO particle is expected to have good long-term stability, because whose growth during heating is inhibited by the LSCN and CeO_2 grains. The influence of Ni-substituted $LaCrO_3$ on the properties of the anode were researched [13–15]. Thermodynamic calculations represented the Ni substitution destabilized the system; experimentally, nickel metal-substituted $LSCrO_3$ did not decompose readily in the reducing atmosphere indicating that the demixing is at least kinetically hindered. In this experimental, we can speculate that a little Ni substitution does not destabilize the system.

Shown in Fig. 7 are shrinkage characteristics of LSCCN sample after pre-calcining at 1450 °C for 5 h. In the range of 30–800 °C, the TEC value is $11.8 \times 10^{-6}\,K^{-1}$, which is close to that of YSZ ($10.8 \times 10^{-6}\,K^{-1}$). Therefore, from the viewpoint of thermal expansion, we have designed the composite material, which has a matching TEC with the YSZ electrolyte as well as showing linear thermal expansion behavior in air.

Fig. 8 shows the temperature dependence of the conductivity of LSCCN samples prepared by calcining at 1450 °C for

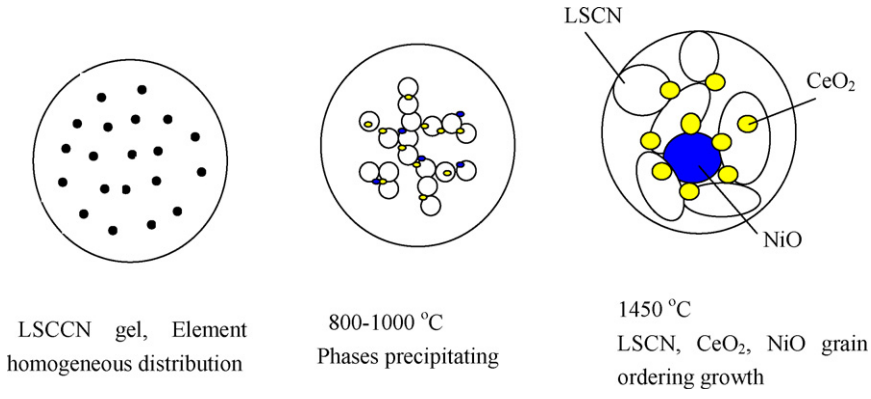

Fig. 6. Schematic of LSCN, CeO_2, and NiO phase formations.

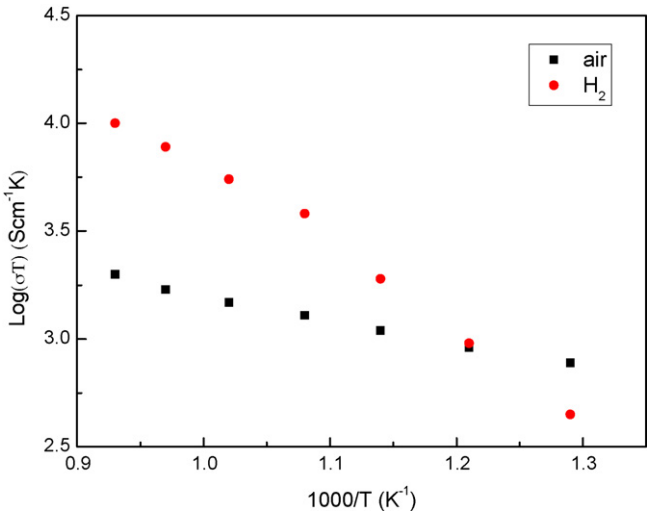

Fig. 8. The temperature dependence of the conductivity of LSCCN samples prepared by calcining at 1450 °C for 5 h.

5 h. Results show that the electrical conductivity of LSCCN in $H_2 + 3\%$ H_2O is obviously higher than that in air above 600 °C. At 800 °C, the conductivities are 1.84 S cm^{-1} in air and 5.03 S cm^{-1} in an $H_2 + 3\%$ H_2O atmosphere, respectively. For the doped $LaSrCrO_3$, the conductivity in air was higher than in hydrogen. In the case of such p-type conductors, the conductivity decreases in reducing atmosphere because of the decrease of charge carriers (holes) in combination with an increase of oxygen vacancies [16]. The LSCCN has higher conductivity in reducing atmosphere due to the fact that, at reducing atmosphere, the Ce^{4+} ion of CeO_2 can be reduced to Ce^{3+} as well as NiO is reduced into metallic Ni. This may be an attractive property for the use of LSCCN for an anode in SOFC.

Cell voltage and power density for a single cell with an YSZ electrolyte of about 350 μm thickness as a function of current density are shown in Fig. 9. The power density of the single cell with a LSCCN anode and a LSM/YSZ cathode is 135 mW cm^{-2} in an $H_2 + 3\%$ H_2O atmosphere at 800 °C, which is obviously lower than that of the single cell with Ni–YSZ

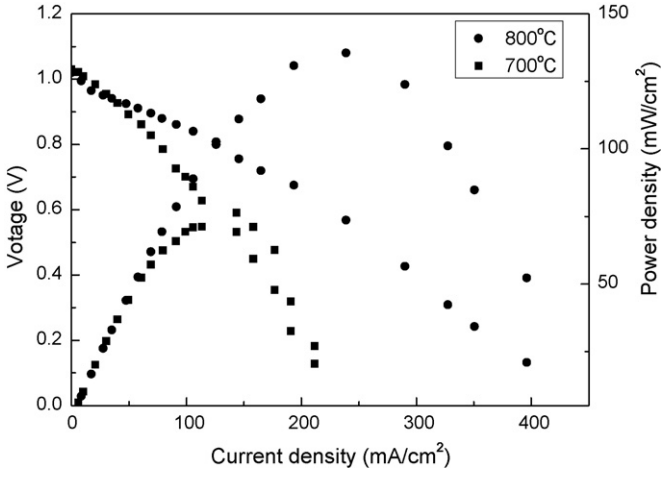

Fig. 9. Cell voltage and power density for a single cell with an YSZ electrolyte of about 350 μm thickness as a function of current density.

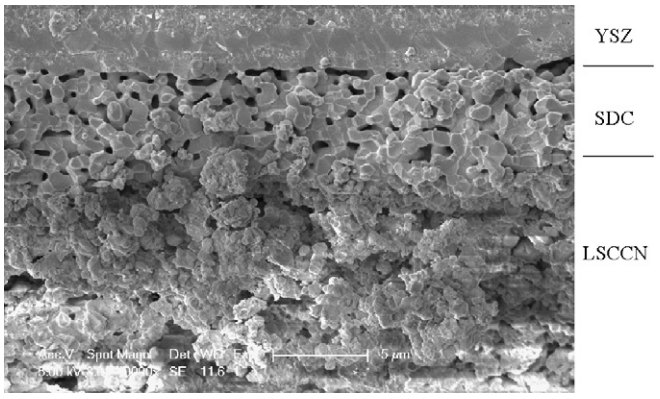

Fig. 10. The section morphologies of single cells after testing in an $H_2 + 3\%$ H_2O atmosphere from 500 to 800 °C.

anode and LSM/YSZ cathode, which is 1945 mW cm^{-2} in an $H_2 + 3\%$ H_2O atmosphere at 800 °C [17], although the standard open circuit potential was observed. In this experimental, the power density is very stable during 100 h at 800 °C. The section morphologies of a single cell is shown in Fig. 10, in which the YSZ electrolyte with about 350 μm thickness and a porous SDC interlayer with about 6.5 μm thickness, which was prepared by pressing the YSZ powder into a Ø15 mm pellet and SDC slurry was coated on the both sides of the YSZ pellets and then co-calcined at 1400–1450 °C for 5 h. From Fig. 10, the SDC interlayer was used to decrease the interfacial resistances between electrode and electrolyte. It is observed that the anode has a poor porosity. The cell performance was not well characterized because of the low porosity for this anode and the thick YSZ electrolyte, which has a high ohmic resistance. Therefore reducing the electrolyte ohmic resistance and improving the anode microstructure is expected to improve the cell performance to a desirous level.

4. Conclusion

A new anode material has been synthesized using an auto-ignition process with a general formula of $(La_{0.7}Sr_{0.3})_{1-x}Ce_x$-$Cr_{1-x}Ni_xO_3$. It shows a unique structure with the fine CeO_2 and Ni grains highly dispersed on the $La_{0.7}Sr_{0.3}Cr_{1-x}Ni_xO_3$ that formed a skeleton. At 800 °C, the electric conductivity measurements show that the conductivity is 1.84 S cm^{-1} in air and 5.03 S cm^{-1} in an $H_2 + 3\%$ H_2O atmosphere. The maximum power density is 135 mW cm^{-2} in an $H_2 + 3\%$ H_2O atmosphere at 800 °C. More work is needed to improve the electrochemical behavior of these anodes, evaluate their long-term stability, determine their performance in different fuels, evaluate reduction–oxidation cycling performance, and observe effects of sulfur contamination.

Acknowledgments

This work was supported by the Natural Science Foundation of Education Department of Anhui province under contract no. 2006KJ126B and no. KJ2007A125ZC.

References

[1] N.Q. Minh, Solid State Ionics 174 (2004) 271–277.
[2] S.M. Haile, Acta Mater. 51 (2003) 5981–6000.
[3] A. Atkinson, S. Barnett, R.J. Gorte, J.T.S. Irvine, A.J. Mcevoy, M. Mogensen, S.C. Singhal, J. Vohs, Nature Mater. 3 (2004) 17–27.
[4] S. Park, J.M. Vohs, R.J. Gorte, Nature 404 (2000) 265–267.
[5] S.W. Tao, J.T.S. Irvine, Nature Mater. 2 (2003) 320–323.
[6] O.A. Marina, N.L. Canfield, J.W. Stevenson, Solid State Ionics 149 (2002) 21–28.
[7] B.D. Madsen, S.A. Barnett, J. Electrochem. Soc. 154 (6) (2007) B501–B507.
[8] B.D. Madsen, S.A. Barnett, J. Electrochem. Solid-State Lett. 154 (6) (2007) B501–B507.
[9] J. Liu, B.D. Madsen, Z.Q. Ji, S.A. Barnett, J. Electrochem. Solid-State Lett. 5 (6) (2002) A122–A124.
[10] S.Q. Hui, A. Petric, J. Eur. Ceram. Soc. 22 (2002) 1673–1681.
[11] A.L. Sauvet, J.T.S. Irvine, Solid State Ionics 167 (2004) 1–8.
[12] E.P. Murray, T. Tsai, S.A. Barnett, Nature 400 (1999) 649–651.
[13] J. Sfeir, J. Power Sources 118 (2003) 276–285.
[14] A.L. Sauvet, J. Fouletier, F. Gaillard, M. Primet, J. Catal. 209 (2002) 25–34.
[15] J. Sfeir, P.A. Buffat, J. Catal. 202 (2001) 229–244.
[16] I. Yasuda, M. Hishinuma, Solid State Ionics 80 (1995) 141–150.
[17] S.D. Souza, S.J. Visco, L.C.D. Jonghe, Solid State Ionics 98 (1997) 57–61.